Magnet Design and Construction for EMMA

Ben Shepherd[a*]

[a]*ASTeC, STFC Daresbury Laboratory, Warrington WA4 4AD, UK*

Abstract. EMMA is a 20 MeV non-scaling Fixed Field Alternating Gradient accelerator (nsFFAG) proof-of-principle prototype, to be built at Daresbury Laboratory in the UK as an accelerator physics experiment to explore the behaviour of such machines. The magnet designs present major challenges - the lattice is made up of 84 quadrupoles, with different horizontal offsets from the magnet centres in the focusing and defocusing quads. These offsets alone provide the necessary bending fields in the ring. The magnets are also very thin (55mm and 65mm yoke lengths) and end field effects therefore dominate. Careful design, followed by prototype construction and measurement, is essential. The magnets have been designed in 3D from the outset, using the CST EM Studio software. The paper will present the results of the design, showing how the magnets have been optimised to improve the integrated good gradient region, and will report on the progress of the prototyping work.

Keywords: EMMA, FFAG, accelerator, magnet, electrons, design, prototype, measurement.

PACS: 41.20.Gz; 41.75.Ht; 41.85.Lc.

INTRODUCTION

The Electron Machine for Many Applications (EMMA) will be a non-scaling Fixed Field Alternating Gradient (nsFFAG) accelerator as an add-on to the Energy Recovery Linac Prototype (ERLP)[1] project at Daresbury Laboratory. EMMA is part of the CONFORM project[2], funded within the BASROC initiative, and is a proof-of-principle machine. It will take a 10MeV beam from the ERLP, accelerate it up to 20MeV in a few tens of turns and extract it into a diagnostic beamline.

EMMA's main lattice magnets are 84 quadrupoles (42 each of F and D types), which are offset to provide a dipole field, and therefore effectively work as combined function magnets. The magnets will be movable in the horizontal direction to provide independent control of the dipole and quadrupole fields.

MAGNET CHALLENGES

Due to the small size of the EMMA ring (16.6m circumference) and the large number of magnets, each magnet is very thin – the yoke thicknesses are the same order as the inscribed radii. The field is therefore dominated by end effects, which in conventional storage ring magnets are small corrections.

The beam will also move significantly inside the vacuum chamber as it is ramped in energy. The required horizontal aperture is therefore rather large, and consequently the good field region specified for the magnets is quite demanding.

The size of the ring is such that all the EMMA components (magnets, cavities, injection/extraction magnets, diagnostics and correctors) must fit into an extremely small space. Interaction between the two magnets in a cell must be taken into consideration, as well as fields in the straight sections.

Full 3D modelling using CST EM Studio[3] has been employed from the outset. A pair of prototype magnets has been built by Tesla Engineering[4], to verify the simulation work.

* Corresponding author: b.shepherd@dl.ac.uk

MAGNET PARAMETERS

Table 1 shows a list of current magnet parameters. The individual magnet profiles are shown in Figure 1. The required good field regions are highlighted with a rounded rectangle in each case. Note that the good field region for the D magnet is entirely offset from the magnetic centre.

TABLE 1. List of current magnet parameters for EMMA.

Parameter	F magnet	D magnet	Units
Integrated gradient	-0.387	0.347	T
Inscribed radius	37	53	mm
Current	350	350	A
Turns in coil	10	15	
Yoke thickness	55	65	mm
Pole width	73	110	mm
Horizontal movement range	-2.711	-5.28	mm
	+2.604	+14.535	
Offset from magnetic centre	7.507	34.025	mm
Required good field region	-32…+16	-56…-10	mm

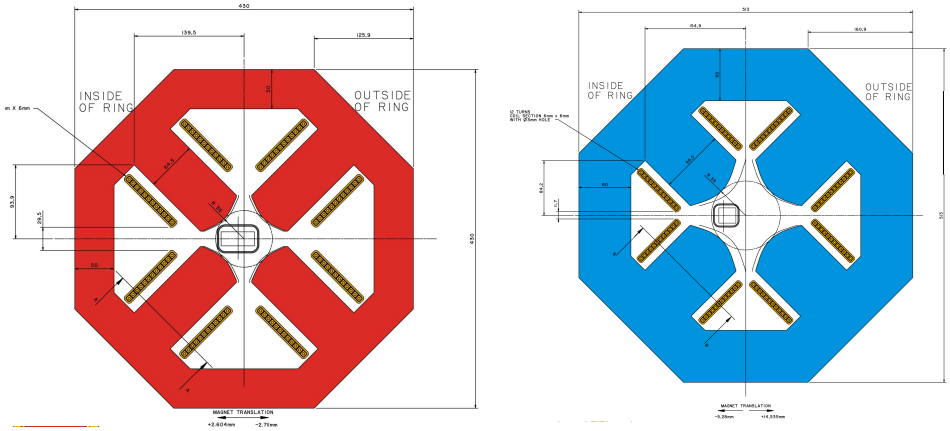

FIGURE 1: Magnet profiles: F (left) and D (right).

MAGNET MODELLING

A 2D model of the F magnet was produced in OPERA, to find a ballpark figure for the **tangent point** – the point at which the pole profile goes from a hyperbolic curve to a tangent. 3D modelling suggested that, due to the very short magnet length, the central gradient was not as high as the 2D model. The length would have to be at least doubled to reach the 'plateau' value (Figure 2). This confirms that the field is dominated by end effects. The central gradient is therefore smaller than that expected from the 2D model; however, the integrated gradient is rather larger than naïvely expected (by multiplying the central value by the yoke length).

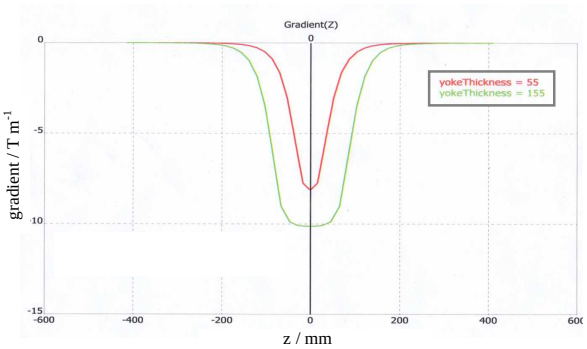

FIGURE 2: Gradient profile through the F magnet using two different values of yoke thickness. The gradient from the 155mm-thick magnet reaches a plateau value, but the 55mm-thick magnet does not.

Interaction between the F and D magnets in a cell was assessed by building three models: two separate models and one with both magnets. The difference (in gradient) between a linear addition of the separate models and the combined model was found to be about 0.25T/m at the centre of the F magnet – about 5% of the central gradient (Figure 3).

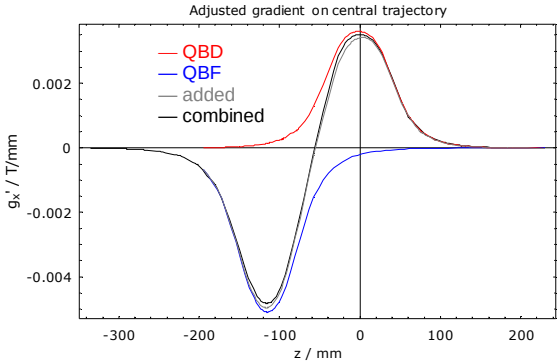

FIGURE 3: Gradient on the nominal 15MeV beam path, showing the two individual magnets (red and blue), a linear superposition of these (grey) and a combined model (black).

The injection line design[5] specifies a kicker that will not be affected by magnetic field from the F and D magnets. To limit the amount of field leaking into the long straight, field clamps were added to the design. Thin (5mm) steel plates with a hole for the vacuum chamber will be added on either side of every F-D pair, providing a return path for the stray magnetic flux and decreasing the field in the long straight to acceptable levels.

Each magnet was optimised separately in EM Studio, with a view to tweaking the combined model at a later stage and providing a field map to use in tracking studies, iterating the design further. The goal was to achieve as large a possible region within which the integrated gradient variation did not exceed ±0.1%. The design goals were specified as ±32mm for the F magnet and ±56mm for the D magnet. These apertures are defined by the required beam movement as the energy changes, plus the horizontal movement specified for each magnet.

Initially, two variables were used in the simulation – tangent point and the size of the chamfer at the pole ends. For a normal (long) storage ring quadrupole, this would give sufficient degrees of freedom – adjusting the tangent point to correct the central field, and then adding a chamfer to correct for end effects. However, in these very short magnets, the end fields dominate the overall field quality, and the gradient map seems to have features which cannot be corrected for using these variables alone. The maximum good field region available using this geometry (including a field clamp) was ±14mm.

A new approach was tried, changing from the old pole face model that used a hyperbolic section and a tangent section.

‘Straight-Line’ Pole Geometry

An arbitrary pole design provides the freedom to adjust the field profile with fewer restraints than that imposed by a ‘traditional’ quadrupole design. However, it raises the question of how to parametrise the pole. The model initially tried was based on the following steps (see Figure 4 for definition of parameters):

- Begin with a square pole.
- Remove material from each side of the pole, adjusting the d_0 point until reaching an optimum.
- Adjust the d_1 point, halfway between the pole centre and the side.
- Introduce a third (d_2) point halfway between the two previous points, and adjust this.

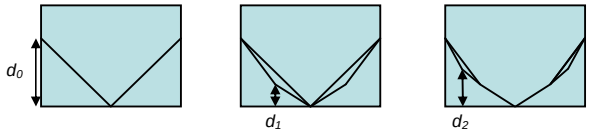

FIGURE 4: Optimisation of straight-line geometry for an even number of pole tip facets. Points are introduced one at a time, optimising at each step.

This method turns out to be very successful in generating a pole geometry that conforms to the specification. Without field clamps, the good field region in the F magnet was extended to ±32mm. Adding the field clamp to the model, however, has an adverse effect on the field quality.

The shape of the vacuum window in the field clamp was altered to try to improve the field quality. Various different shapes were tried (Figure 5), but the best was found to be a shape following the outline of the magnet poles. This has the advantage of keeping the quadrupole symmetry, so that field quality in the vertical direction does not require further evaluation.

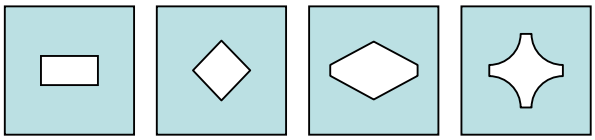

FIGURE 5: Differing vacuum window shapes in the field clamp: (from left to right) rectangle, diamond, tapered rectangle, and following the pole shape.

A variant of the straight-line pole tip geometry was tried in which an odd number of pole tip faces were used. Designs with three and five faces, using one and two variables respectively, were tried out (Figure 6). The optimisation was done sequentially as above, based on the assumption that the two variables were fairly orthogonal.

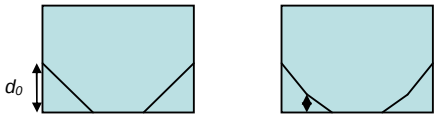

FIGURE 6: Optimisation of straight-line geometry for an odd number of pole tip facets (three and five).

For the F magnet, the best result was found for a five-face geometry with d_0 = 19.5mm and d_1 = 4.25mm, resulting in a good field region of ±22.9mm (Figure 7). This is somewhat short of the specified value of 32mm. It may become clearer whether this could be acceptable or not when tracking studies are carried out using real simulated field maps from this study.

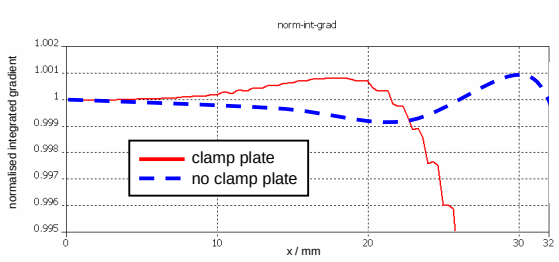

FIGURE 7: Normalised integrated gradient plot of the optimum configuration for the F magnet. The good field region is 22.9mm. A plot for a magnet with no clamp plate is also shown.

MAGNET PROTOTYPES

A full prototype of both types of magnet was built by Tesla Engineering. The strength and field quality of the magnets was measured using a rotating coil bench[6]. In the case of quadrupoles, this method allows several variables to be determined:

- the gradient strength of the magnet;
- the transverse distance of the coil from the magnetic centre;
- the angle of the coil relative to the magnet;
- the field quality in terms of higher harmonics.

Using the field harmonics extracted from this data, it is possible to reconstruct the integrated field profile, and to calculate the good gradient region of the magnet.

The results from these tests are shown in Table 2. The normalised integrated gradient profiles, as reconstructed from the harmonic data, are shown in Figure 8.

TABLE 2. Results of measurements of the prototype magnets.

Parameter	**F model**	**F spec**	**F measured**	**D model**	**D spec**	**D measured**	**Units**
Current	350	364	350	350	376	350	A
Turns	10	10	10	15	15	15	turns
Current turns	3500	3640	3500	5250	5640	5250	At
Gradient at magnetic centre	-6.583	3.71		4.603	3.71		T/m
Integrated central gradient	0.585	0.483	0.540	0.515	0.440	0.480	T
Good field region (±0.1%)	10.2	32.0	15.0	32.2	56.0	21.0	mm`
Gradient uniformity	2.80%		0.43%	0.11%		10.2%	
out to	36.0		30.5	32.2		56.0	mm

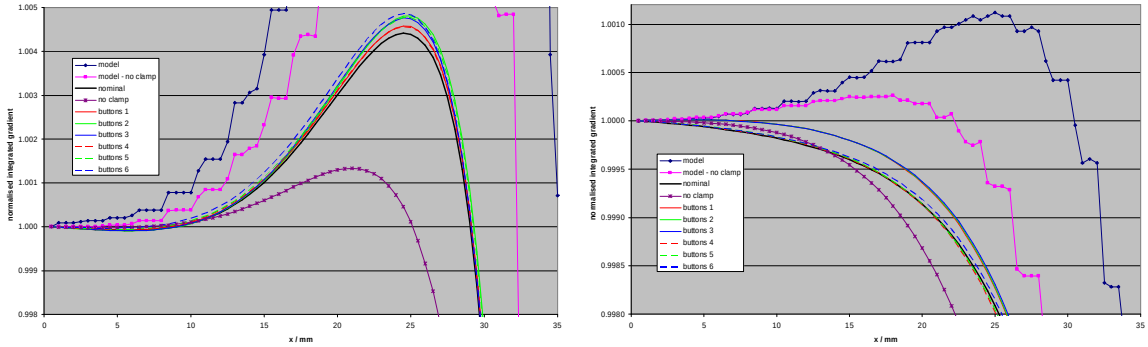

FIGURE 8. Normalised integrated gradient profile for the F (left) and D (right) magnet prototypes.

In both cases, the gradient drops off quicker with distance from the magnetic centre than the model predicts. For the F magnet, this has the effect of improving the field quality – the gradient variation is about 0.4% within the specified 32mm good field region. However, for the D, the measured field quality is somewhat lower than expected; the gradient drops off by about 13% at 56mm.

Extra Tests

Further tests using the rotating coil bench were carried out on each magnet.

The strength of the production magnets will be adjustable by varying the longitudinal position of the clamp plate. This was tested in the prototypes by moving the clamp plate by up to 1mm in either direction. For the F, a movement of 1mm resulted in a 0.25% increase in strength; this should provide adequate adjustment. However, for the D, the strength did not change at all. The reason for this is possibly some saturation in the clamp plate. This could be mitigated by increasing the thickness of the clamp plate.

Steel 'buttons', 5mm in diameter, were added to the ends of the poles, in several places (Figure 9). This was intended to show that the harmonics could be modified. There was a small effect on the field harmonics but bigger pieces of steel would be required for any significant effect.

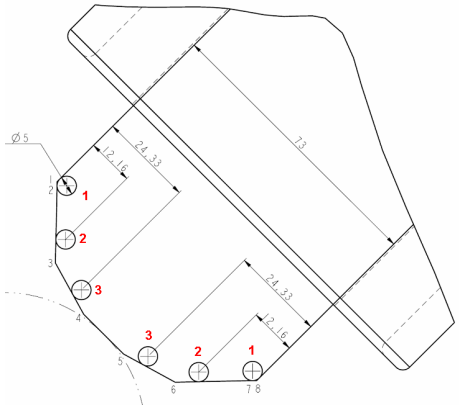

FIGURE 9. Positions of steel buttons added to the magnets.

Model Comparisons

The model and the field measurements do not match up very well. The harmonics predicted by the model are rather different, and the good field region is significantly smaller than that in the model. Some work is required to reconcile these differences. Some initial modelling using OPERA-3D[7] has been carried out in conjunction with Tesla, and the results are promising. This work should be continued.

FURTHER WORK

The magnet measurements at Tesla will continue. The magnets in the ring will be located in close proximity to each other, and it is important to ascertain how the fields interact. The magnets will be placed on the rotating coil bench at the same time and measured together.

In light of the poor field quality in the D magnet, some shimming work will be done to try and improve the field. The 'straight-line' pole face design means that it is quite easy to add steel shims.

Modelling will be carried out using an alternative simulation package (OPERA, as mentioned above). The results from modelling and from measurements should be fed into an accelerator physics simulation of the entire machine to assess the performance of the magnets, and identify how they could be improved further.

The tender exercise for the production magnets will go ahead via a European Journal (OJEU) contract; the specification has been published, and a manufacturer is expected to be announced at the end of 2007. Further magnet design work will go ahead in parallel with this procurement exercise.

CONCLUSIONS

The specific requirements of this machine – the world's first non-scaling FFAG – mean that these are very challenging magnets to design. The usual method of designing a quadrupole – a hyperbolic pole face – has been rejected in favour of a 'straight-line' pole design, which produced improved field quality over the normal design. This is due to the small aspect ratio of these magnets, and the large aperture over which the gradient is required to be uniform.

Prototypes of the magnets have been built and tested, and further measurements will be carried out as well as further design work. Though the D magnet did not perform as well as expected, it should be possible to produce magnets that meet the demanding specification for this machine. The production magnets will be built, tested and delivered to Daresbury Laboratory by the summer of 2008.

ACKNOWLEDGMENTS

The author would like to thank Neil Marks for his invaluable support and advice during this magnet design process. Neil Bliss and Clive Hill provided engineering support and drawings. The author is also grateful to the staff at Tesla Engineering, particularly Martin Crawley for carrying out the field measurements, and Fred Goldie for his OPERA modelling expertise.

REFERENCES

1. S.L. Smith, "The Status of the Daresbury Energy Recovery Linac Prototype", PAC 2007 (TUPMN084).
2. R.J. Barlow, "The CONFORM Project: Construction of a Nonscaling FFAG and its Applications", PAC 2007 (THPMN078).
3. CST simulation software, www.cst.com.
4. Tesla Engineering, www.tesla.co.uk.
5. T. Yokoi & S. Machida, "Beam Injection into EMMA Non-Scaling FFAG", PAC 2007 (THPMN082).
6. R.P. Walker, 'Magnetic Measurements', in H. Winick, 'Synchrotron Radiation Sources: A Primer', World Scientific, 1994, p181-188.
7. OPERA simulation software, www.vectorfields.com.